Available online at www.sciencedirect.com

ScienceDirect

journal homepage: www.elsevier.com/locate/he

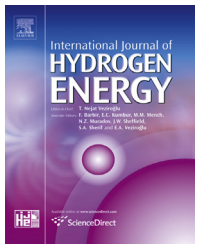

Coexpression of Mo- and Fe-nitrogenase in *Rhodobacter capsulatus* enhanced its photosynthetic hydrogen production

Honghui Yang [a,b,*], *Jing Zhang* [a], *Xueqing Wang* [b], *Jiangtao Feng* [b,*], *Wei Yan* [a], *Liejin Guo* [b]

[a] *Department of Environmental Science & Engineering, Xi'an Jiaotong University, Xian 710049, PR China*
[b] *State Key Laboratory of Multiphase Flow in Power Engineering, Xi'an Jiaotong University, Xian 710049, PR China*

ARTICLE INFO

Article history:
Received 19 August 2014
Received in revised form
1 November 2014
Accepted 17 November 2014
Available online 9 December 2014

Keywords:
mopAB deletion
Fe nitrogenase
Nitrogenase activity
Hydrogen production

ABSTRACT

The effects of *mopAB* disruption in *Rhodobacter capsulatus* SB1003 on the nitrogenase expression level, activity and photo-fermentative hydrogen production were studied. The results showed that the disruption of *mopAB* derepressed the expression of Fe nitrogenase and showed no negative effect on the expression of Mo–Fe nitrogenase. The nitrogenase activity of YMP1 (*mopAB*$^-$) was 4.22 ± 0.30 nmol acetylene/(min·mg-dcw), which was higher than that of 2.97 ± 0.20 nmol acetylene/(min·mg-dcw) obtained from the wild type strain SB1003. The hydrogen yields of YMP1 were enhanced by 26.7%, 39.7% and 35.3% compared with those obtained from SB1003 under the light intensity of 2500 lux, 5000 lux and 8500 lux respectively. The maximum hydrogen production rates of YMP1 were enhanced by 14.5%, 15.1% and 24.1% compared with those of SB1003 under the same condition. The results suggest that expressing nitrogenase related genes could be an alternative way for improving the hydrogen production performance of purple non-sulfur bacteria.

Introduction

Purple non-sulfur bacteria (PNSB) are studied for its capability on hydrogen production from renewable resources [1–6]. In order to enhance the photo-fermentative hydrogen production performance of PNSB, several strategies were employed to manipulate the metabolism pathways [7,8], including deactivating the hydrogen uptake pathway by knocking out the *hupSLC* genes [9], and deactivating the polyhydroxybutyrate (PHB) synthesis pathway by disrupting the *phbC* gene [10,11]. These strategies were focused on enhancing the redistribution of reductant to nitrogenase.

Nitrogenase is significant for photosynthetic hydrogen generation with PNSB. The activity of nitrogenase is positively related with the hydrogen production performance of PNSB [6,12]. The disruption of *hupSL* genes resulted in enhanced nitrogenase expression level and nitrogenase activity [13], which could be the reason of the enhanced

* *Corresponding authors*. Department of Environmental Science & Engineering, Xi'an Jiaotong University, Xian 710049, PR China. Tel.: +86 29 82664731.
E-mail addresses: yanghonghui@mail.xjtu.edu.cn (H. Yang), fjtes@mail.xjtu.edu.cn (J. Feng).
http://dx.doi.org/10.1016/j.ijhydene.2014.11.087

hydrogen production performance of *hupSL*$^-$ mutant. Disruption of *ccoNOQP* genes from *Rhodobacter capsulatus* SB1003 also enhanced the nitrogenase expression level, and enhanced the hydrogen production rate and hydrogen yield clearly [4,14]. Therefore, enhancing nitrogenase expression level could improve the hydrogen production performance. In *R. capsulatus*, there is an alternative nitrogenase that is silent in the presence of soluble molybdenum and *mopAB* genes and, which are two molybdenum dependent regulators inhibiting the expression of alternative nitrogenase in the presence of molybdenum [15,16]. In this case, the mutant with interrupted *mopAB* genes could express alternative nitrogenase and Mo-nitrogenase simultaneously in *R. capsulatus*. It was reported that the alternative nitrogenase was naturally more favorable for hydrogen production than Mo-nitrogenase during nitrogen fixation according to the equations showed in literature [17], in which the H_2 to NH_3 ratio is 9 folds compared to that obtained in equation catalyzed by Mo-nitrogenase. But little is known about the hydrogen production with alternative nitrogenase, and applying the alternative nitrogenase for hydrogen evolution would benefit the understanding on hydrogen generation with PNSB and may offer some clue for genetic modification of PNSB based on hydrogen production rate and yield. In this study, the genes *mopAB* were disrupted to implement the co-expression of Fe-nitrogenase and Mo-nitrogenase, and the effects of *mopAB* disruption on hydrogen production performance of the corresponding mutants under different light intensity were studied. The limitation factors for hydrogen production performance under different light intensity were also discussed.

Material and methods

Bacterial strains and growth conditions

The bacteria including *R. capsulatus* and *Escherichia coli* strains used in this work are listed in Table 1. *R. capsulatus* SB1003 was used as a wild type strain [18].

MPYE [19] and modified Sistrom's mineral media [20] were employed to culture *R. capsulatus* SB1003 and its mutants. Modified Sistrom's mineral media (MedA) was prepared by substituting the succinate with 25 mM acetic acid and 30 mM butyric acid. Luria–Bertani liquid medium (LB) supplemented with proper amount of antibiotics was used to incubate *E. coli* strains carrying plasmids. For pre-culture of *R. capsulatus* and *E. coli* strains, 10 mL MPYE or LB medium was filled into 50 mL sterile screwed tubes and incubated in 35 °C (for *R. capsulatus* strains) or 37 °C (for *E. coli* strains) incubators. Antibiotics were supplemented at the following concentrations: ampicillin 100 mg/L, kanamycin 50 mg/L, gentamycin 12 mg/L for *E. coli* culture and kanamycin10 mg/L, gentamycin 12 mg/L, rifampicin 200 mg/L for *R. capsulatus* culture, respectively.

Construction of plasmids and mutants

As shown in Fig. 1(a), the *mopAB* region of SB1003 with around 500 bp flank sequences was amplified with primers SenseP-*Xba*I-(AAG TCT AGA GGC ACC GGC CTT GCG CTG GAT CTT T), and AntisenseP-*Kpn*I-(AAT GGT ACC TTT TCA GCA CCG CGC CCT TGT CAT C) by PCR and the fragment was cloned into pBlu2SKP via *Kpn*I and *Xba*I sites to obtain the plasmid

Table 1 – –Bacterial strains and plasmids used in this study.

	Genotype	Ref.
E. coli Strains		
HB101	*hsd*S20, *xyl*5, *λ*$^-$, *rec*A13, *gal*K2, *ara*14, *sup*E44, *lac*Y1, *rps*L20(str^r), *leu*B6	Stratagene
S17-1 λpir	TpR SmR *rec*A, *thi*, *pro*, *hsd*R-M + RP4: 2-Tc:Mu: Km Tn7 *λpir*	Stratagene
R. capsulatus		
SB1003	Rif-10 Rif^R	[18]
YMP1	*mopAB*$^-$ of SB1003	This study
YMP7	(*mopAB*$^-$, *nifHD*$^-$) of SB1003	This study
YMP10	(*mopAB*$^-$, *anfA*$^-$) of SB1003	
Plasmids		
pRK2013	Helper plasmid, Km^r	[21]
pZJD29c	Eliminate *Kpn*I site in *sacB* gene of pZJD29a by site directed mutagenesis, *oriR6K*, *sacB*,Gen^r	[26]
pBlu2SKP	Amp^r	Stratagene
pXCA601	Tet^r	[22]
pBBR1MCS-2	Km^r	[27]
pYNB02	Km^r, *lacZ*	This study
pAnfH01	*lacZ* fusion with *anfH* gene promoter	This study
pNifH01	*lacZ* fusion with *nifH* gene promoter	[4]
pNifH1/pAnfH1	pBlu2SKP derivate containing *nifHD/anfAH*	This study
pNifH2/pAnfH2	pNifH1 derivate with deletion between *Bam*HI sites; pAnfH2 derivate with deletion between *Sma*I and *Stu*I sites	This study
pNifH6/pAnfH6	pZJD29c derivate carrying mutated *nifHD/anfA*	This study
pMP1	pBlu2SKP derivate containing *mopAB*	This study
pMP2	pMP1 derivate with deletion between *Stu*I	This study
pMP3	pZJD29c derivate carrying mutated *mopAB*	This study

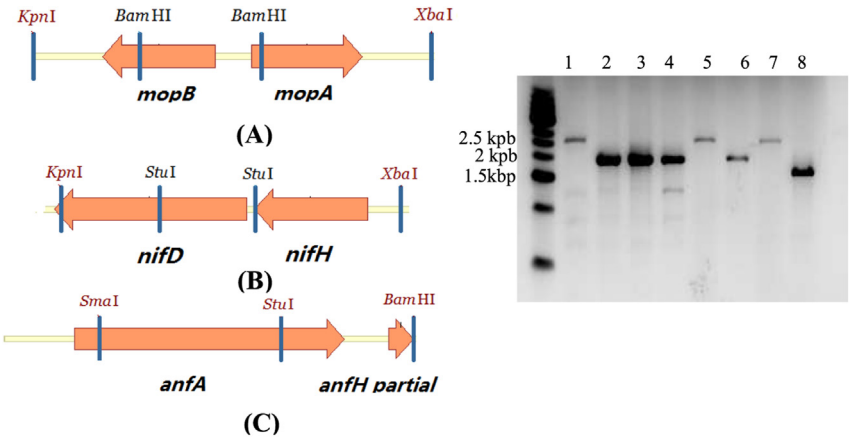

Fig. 1 – Scheme for partial deletion of *mopAB* via *Bam*HI sites (A), the scheme for partial deletion of *nifHD* via *Stu*I sites (B), and the scheme for partial deletion of *anfA* gene(C); the gel patterns showed the PCR results of the corresponding regions before and after deletion. Lane 1–4: *mopAB* region from SB1003, YMP1, YMP7 and YMP10; Lane 5 and 6: *nifHD* region from SB1003 and YMP7; Lane 7–8: *anfA* region from SB1003 and YMP10.

pMP1(ampicillin resistance, selected in LB media plus 100 mg/L ampicillin, and the obtained plasmids were identified by restriction enzyme digestion using *Kpn*I and *Xba*I). The pMP1 was digested with *Bam*HI restriction enzyme and the large fragment was ligated with T4 DNA ligase to obtain pMP2, which contained the *mopAB* DNA sequences with deletion between the two *Bam*HI sites (The deletion was confirmed by restriction enzyme digestion using *Bam*HI). The DNA fragment containing *Bam*HI deletion from pMP2 was then ligated into a suicide plasmid pZJD29c (Gentamycin resistance) via *Kpn*I and *Xba*I sites to obtain a new plasmid pMP3. This plasmid was primary selected with LB media plus 12 mg/L gentamycin, and the obtained candidates were identified with restriction enzymes digestion using *Kpn*I and *Xba*I. The recombinant plasmid pMP3 was constructed for the disruption of *mopAB* genes.

The *nifH-nifD* fragment of SB1003 was amplified with the primers SND-*Xba*I-(AAG TCT AGA AAC CGC CGC AAG GAC CGG AAA ACCC), and ASND-*Kpn*I-ASND- (AAT GGT ACC CAG ACG GGG TTG TTG ATC GCC ATGT), and it was cloned into pBlu2SKP with *Kpn*I and *Xba*I sites to obtain new plasmid pNifH1. The pNifH1 was digested with restriction enzyme *Stu*I to create a deletion between *Stu*I sites, and the large fragment was ligated to obtain a plasmid pNifH2. The fragment containing a deletion in *nifH* and *nifD* from pNifH2 was then cloned into a suicide plasmid pZJD29c via *Kpn*I and *Xba*I sites to create a new derivate pNifH6. The selection and identification procedures of pNifH1, pNifH2 and pNifH6 were similar with those for pMP1, pMP2 and pMP3, respectively. The recombinant plasmid pNifH6 was constructed for the disruption of *nifHD* genes.

The *anfA-anfH* DNA fragment of SB1003 with the primers: SenseA-(ATA CTG CAG GTC GTT TCG GCC ACC AGC CGC AACA) and ASPH-(ATA GGA TCC AGG ATC AGC CGG GTG CTG TCG GCT T), and ligated the fragment into pBlu2SKP by *Bam*HI and *Sma*I sites to obtain pAnfH1 plasmid. The pAnfH1 plasmid was digested with *Sma*I and *Stu*I, and religated the largest fragment to obtain a new plasmid named pAnfH2. The *Kpn*I-*Xba*I fragment carrying the fragment of *anfA-anfH* was ligated into pZJD29c with the same sites to obtain a suicide plasmid pAnfH6. Again, the selection and identification procedures of pAnfH1, pAnfH2 and pAnfH6 were similar with those for pMP1, pMP2 and pMP3, respectively. The recombinant plasmid pAnfH6 was constructed for the disruption of *anfA* gene.

Tri-parental cross assisted by pRK2013 was employed for creating the mutations on *mopAB*, *nifHD* and *anfA* genes [21]. The procedure for knocking out *mopAB*, *nifHD* and *anfA* genes was the same as shown in our previous report [4]. In brief, mutant YMP1 with mutation on *mopAB* was obtained by conjugating *R. capsulatus* SB1003 with pMP3/S17-1, and mutant YMP7 with double mutations on both *mopAB* and *nifHD* was created by conjugating YMP1 with pNifH6/S17-1. Mutant YMP10 with deletions on *mopAB* and *anfA* genes was created by conjugating pAnfH6 with YMP1. All of DNA fragments containing the mutations were confirmed by PCR reactions with the same primers used for cloning described above, and the electrophoresis gel pattern is shown in Fig. 1.

Construction of lacZ *fusion with* nifH *and* anfH *promoters*

The construction procedure of *lacZ::nifH* fusion carrying plasmid was similar with that described in our previous report [4]. The *Hin*dIII-*Bam*HI fragment of pXCA601 containing *lacZ* gene was cloned into pBBR1MCS-2 via *Hin*dIII and *Bam*HI site to construct a new plasmid pYNB02 carrying the *lacZ* fragment [22]. The DNA fragment of *nifH* promoter was amplified by PCR using primer SND-1-*Bam*HI-(ATA GGA TCC TTG GGG TCG CAG CCG ACG ATG AGG AT) and primer NHZ-*Xba*I-(AAG TCT AGA CGC CGC AAG GAC CGG AAA ACC CC), and the obtained 392 bp fragment was ligated into pYNB02 via *Xba*I-*Bam*HI sites to construct pNifH01. The DNA fragment of *anfH* promoter was amplified by PCR using primer SPH-*Xba*I-(AAG TCT AGA CCC TCG CTG CAG ACG GCG CGC GAAA) and primer ASPH-*Bam*HI-(ATA GGA TCC AGG ATC AGC CGG GTG CTG TCG GCTT), and the obtained 731 bp fragment was ligated into pYNB02 via *Xba*I-*Bam*HI sites to construct pAnfH01 that carried the *lacZ::anfH* fusion. All of the obtained plasmids were sent to

Sangon Biotech. Co. for sequencing, and all of the results showed the sequences were identical to the data in Genbank.

Photosynthetic hydrogen production procedure

The modified Sistrom's mineral medium (MedA) was used for pre-culturing *R. capsulatus* SB1003, YMP1, YMP7 and YMP10. Before liquid incubation, the strains were streaked from glycerol stocks onto MedA agar plates and incubated at 35 °C incubator for 3 days, and single colonies from the plates were inoculated into 10 mL MedA liquid in 50 mL screwed tubes and incubated in 35 °C shaker for 48 h. The cultures were harvested by centrifuge and washed twice with fresh MedA liquid medium to neutralize the pH value of the cultures. The harvested bacteria were then re-suspended with proper amount of MedA to prepare the inoculation culture with OD_{660} (optical density at 660 nm) around 0.50, the inoculation culture was mixed with fresh MedA liquid at a ratio of 1–9 for photosynthetic hydrogen production. Sterile 30 mL syringes were employed as photo-reactors and 10 mL of culture was filled in each syringe. All of the photo-reactors were placed in a photo-incubator illuminated by tungsten lamps, and the illumination intensities were set at 2500 ± 300 lux, 5000 ± 300 lux and 8500 ± 500 lux, respectively.

Enzyme assays and measurement methods

The plasmids, pNifH01 and pAnfH01, which carried *nifH::lacZ* fusion and *anfH::lacZ* fusion respectively, were conjugated into SB1003, YMP1 and YMP10 to obtain the strains listed as follows: SB1003/pNifH01, SB1003/pAnfH01, YMP1/pNifH01 and YMP1/pAnfH01, YMP10/pNifH01, YMP10/pAnfH01 for determining the expression levels of *anfH* gene and *nifH* gene by β-galactosidase assay.

The expression levels of nitrogenases were positive related with the activity of β-galactosidase, which is the product of *lacZ* gene fused with *nifH* or *anfH* genes. The activity of β-galactosidase was assayed according to the procedure described in our previous report [4]. The activities of nitrogenases in wild type and mutant strains were assayed with the acetylene reduction method described in literature [4].

Analytical methods

The components of biogas samples were determined by a gas chromatograph (GC, SP2100, Beifen Co. Ltd) equipped with a 4 m × 3 mm stainless column filled with hayesep padding. The liquid components of the photo-fermentative effluents were determined by a GC equipped with a 30 m × 0.32 mm quartz column coated with terephthalic acid modified PEG (AT.FFAP) and a flame ionization detector. The COD values of the photo-fermentative effluents were tested by a COD detector (Lovibond, ET99722). For determining the COD value of the bacterial biomass, a proper amount of culture was assayed on the COD detector for obtaining the total COD value of the culture, and the COD value of the effluent was determined with the effluent after removing the bacteria by filtration using membrane filter with pore size of 0.22 μm in diameter. Therefore, the COD equivalent value (COD_{eq}) of the bacterial biomass in different culture could be calculated by subtracting the COD value of effluent with total COD value. The light intensity between the wavelength of 300 nm and 1000 nm in the unit of mW/m^2 was determined by a photometer (FZ-A, Beijing Normal University Optician), and the irradiation intensity in the unit of lux was detected by a photo-meter (TES1330A, TES Electrical Electronic Co.).

Data analysis

All of the tests were carried out no less than three times and the data showed in this study consisted of average datum ± standard error. The biogases were collected under normal conditions (30 °C and 1 atm), and the volumes data showing in this study were calculated into the data in standard condition (273.15 K, 100 kPa). The hydrogen production profiles were simulated by modified Gompertz equation [23].

Results and discussion

Confirmation on mutations in mutants

The DNA length of *mopAB* fragment in SB1003 is 2798 bp, and the length of the truncated *mopAB* fragment is 1922 bp. The DNA bands shown in lane1, 2, 3 and 4 were consistent with the above number, indicating the successful truncation of *mopAB* in YMP1, YMP7 and YMP10 mutants. The DNA fragment of *nifHD* amplified from *R. capsulatus* SB1003 is 2692 bp as shown in Fig. 1 lane 5, and the length of truncated *nifHD* region by *StuI* is 1938 bp, which is consistent with the DNA band shown in lane 6 of Fig. 1. The fragment of *anfA* amplified from the wild type strain is 2467 bp as shown in lane 7 in Fig. 1. The length of truncated *anfA* region is 1379 bp as shown in lane 8 of Fig. 1. Notwithstanding the imprecise length of DNA molecules shown in electrophoresis gel, the DNA bands shown in lane1 to lane 8 confirmed that the genotype of YMP1(*mopAB*$^-$), YMP7(*mopAB*$^-$, *nifHD*$^-$) and YMP10(*anfA*$^-$) mutants.

Effect of mopAB disruption on the expression and activity of nitrogenase

The β-galactosidase activity of SB1003/pAnfH01 under photo-fermentative condition was undetectable, and that of YMP1/pAnfH01 was 245 ± 15 μM ONPG-Hydrolyzed/(min·mg-protein) as shown in Table 2. This datum indicates

Table 2 – Expression levels of *anfH* and *nifH* genes in *R. capsulatus* strains.

Strains	Genotype	*lacZ* activity[a]
SB1003/pNifH01	wild type/*nifH::lacZ*	934 ± 22
SB1003/pAnfH01	wild type/*anfH::lacZ*	0
YMP1/pNifH01	*mopAB*$^-$/*nifH::lacZ*	1097 ± 80
YMP1/pAnfH01	*mopAB*$^-$/*anfH::lacZ*	245 ± 15
YMP10/pNifH01	(*mopAB*$^-$, *anfA*$^-$)/*nifH::lacZ*	963 ± 28
YMP10/pAnfH01	(*mopAB*$^-$, *anfA*$^-$)/*anfH::lacZ*	2.5 ± 2

[a] Relative activity among the tests, in the unit of μM ONPG-Hydrolyzed/(min·mg-protein).

that the Fe-nitrogenase was expressed in *mopAB*-disrupted mutants. The disruption of *mopAB* results in constitutive expression of *anfA* gene [15], which is the activator of *anfHDGK* operon. The *nifH* expression level in SB1003 reflected by β-galactosidase activity under the same condition was determined to be 934 ± 22 μM ONPG-Hydrolyzed/(min·mg-protein), and the *nifH* expression level in YMP1 was determined to be 1097 ± 80 μM ONPG-Hydrolyzed/(min·mg-protein), which was slightly higher than that obtained in the wild type strain as shown in Table 2. Wang et al. found that the deletion of *anfA* and *mopAB* genes only show slight negative effect on the activity of conventional Mo-nitrogenase when Mo concentration of the culture is below 1 μmol/L, and no negative effect was revealed when Mo concentration is higher than 1 μmol/L [15]. These data confirmed that the deletion of *mopAB* did not show negative effect on the expression of *nifHDK* operon and the activity of Mo-nitrogenase. In order to verify the effect of *mopAB* deletion on *nifH* expression level, the β-galactosidase activity of YMP10/pNifH01 was assayed and the result showed that it was 963 ± 28 ONPG-Hydrolyzed/(min·mg-protein) as shown in Table 2. This result further proved that the disruption of *mopAB* genes did not affect the expression of Mo-nitrogenase clearly. As shown in Table 2, the expression level of *anfH* gene was negligible in YMP10 that was defective in *anfA* genes. As shown in Table 3, the nitrogenase activity assay conducted by the acetylene reduction method showed that the nitrogenase activity of SB1003 was 2.97 ± 0.20 nmol acetylene/(min·mg-dcw), and it was 4.22 ± 0.30 nmol acetylene/(min·mg-dcw) in YMP1, which was enhanced by 42.1% compared with that obtained in wild type strain. And in YMP7 strain, the Fe-nitrogenase activity was 0.47 ± 0.19 nmol acetylene/(min·mg-dcw). The nitrogenase activity in YMP10, whose genotype is *mopAB*$^-$ and *anfA*$^-$, was 2.85 ± 0.32 nmol acetylene/(min·mg-dcw). These results indicate that the nitrogenase activity of the YMP1 mutant strain was clearly enhanced by co-expressing Mo- and Fe-nitrogenases via disrupting *mopAB* genes. The nitrogenase activity of YMP10 mutant was close to that of wild type strain, and it suggests that the enhanced nitrogenase activity of YMP1 was attributed to the co-expression of Fe- and Mo-nitrogenase, and the disruption of *mopAB* did not show negative effect on nitrogenase clearly. Müller et al. reported that the nitrogenase activity of Fe-nitrogenase determined by acetylene reduction method in vivo was only 12.5%–7% of the Mo-nitrogenase activity [24]. The Fe-nitrogenase activities determined by acetylene in this work were consistent with the previous report [24].

Hydrogen production performance of Mo- and Fe-nitrogenase

Fig. 2 shows the cumulative hydrogen production profiles of SB1003, YMP1, YMP10 and YMP7 under photosynthetic condition. Under low light intensity of 2500 ± 300 lux, the hydrogen yield of SB1003 was 2880 ± 200 mL/L, and it increased by 26.7%–3650 ± 220 mL/L from YMP1, but that of YMP7 was only 320 ± 120 mL/L, as shown in Fig. 2(a). YMP10 (*mopAB*$^-$, *anfA*$^-$), which expressed functional Mo-nitrogenase only, showed similar hydrogen production performance with the wild type strain SB1003. Under the light intensity of 5000 ± 300 lux, the hydrogen yields of SB1003 and YMP1 run up to 3562.5 ± 200 mL/L and 4975 ± 150 mL/L, respectively, and hydrogen yield increased by 39.4% via co-expression of two nitrogenases in YMP1. The hydrogen yield from YMP7 (Fe-nitrogenase only) was only 80 mL/L and YMP10 was showed similar hydrogen production performance with SB1003. When the light intensity was increased into 8500 ± 500 lux, the hydrogen yields from the wild type strain and *mopAB*-disrupted mutant were 4062.5 ± 200 mL and 5500 ± 200 mL, respectively, and the increase ratio of hydrogen yield was 35.4% from YMP1 compared with that of SB1003. The mutant YMP10 was still showed similar hydrogen production yield with that of SB1003. Meanwhile, the hydrogen yield from YMP7 was negligible.

As shown in Table 3, when the light intensity was increased from 2500 ± 300 lux into 5000 ± 300 lux, the maximum hydrogen production rates of SB1003 and YMP1, which were obtained by modified Gompertz equation, increased from 43.2 ± 1.4 mL/(Lh) and 49.5 ± 1.2 mL/(Lh) into 60.1 ± 2.7 mL/(Lh) and 69.2 ± 1.3 mL/(Lh), and it further increased into 65.6 ± 3.8 mL/(Lh) and 81.4 ± 3.3 mL/(Lh) respectively at the light intensity of 8500 ± 500 lux. These data show that at low light intensity, the increase ratios of hydrogen production rates between the wild type strain and *mopAB*-disrupted mutant were only 14.5% at 2500 ± 300 lux and 15.1% at 5000 ± 300 lux, and at the light intensity of 8500 ± 500 lux, the increase ratio of hydrogen production rates was 24.1%. When the light intensity was increased from 2500 ± 300 lux to 5000 ± 300 lux and 8500 ± 500 lux, the increase ratio of hydrogen production rate was reduced from 39.1% to 9.2% in SB1003 culture, which was much less than the increase ratio of light intensity. Especially when the light intensity was up to 8500 lux, the maximum hydrogen production rate was only increased by about 5.5 mL/(Lh). Wang et al. found that the hydrogen production yield and rate achieved maximum at the light intensity of 6000 lux and decreased

Table 3 – Nitrogenase activity of *R. capsulatus* strains and maximum hydrogen production rates.

Strains	Genotype	Nitrogenase activity[b]	2500 lux R_m[a]	5000 lux R_m	8500 lux R_m
SB1003	Wild type	2.97 ± 0.20	43.2 ± 1.4	60.1 ± 2.7	65.6 ± 3.8
YMP1	*mopAB*$^-$	4.22 ± 0.30	49.5 ± 1.2	69.2 ± 1.3	81.4 ± 3.3
YMP10	*mopAB*$^-$, *anfA*$^-$	2.85 ± 0.32	41.7 ± 1.7	57.0 ± 2.2	64.2 ± 3.6
YMP7	*mopAB*$^-$ *nifH*$^-$	0.47 ± 0.19	9.1 ± 1.7	4.7 ± 1.5	0

[a] Maximum hydrogen production rate, mL/(L·h).
[b] nmol acetylene/(min·mg-dry cells).

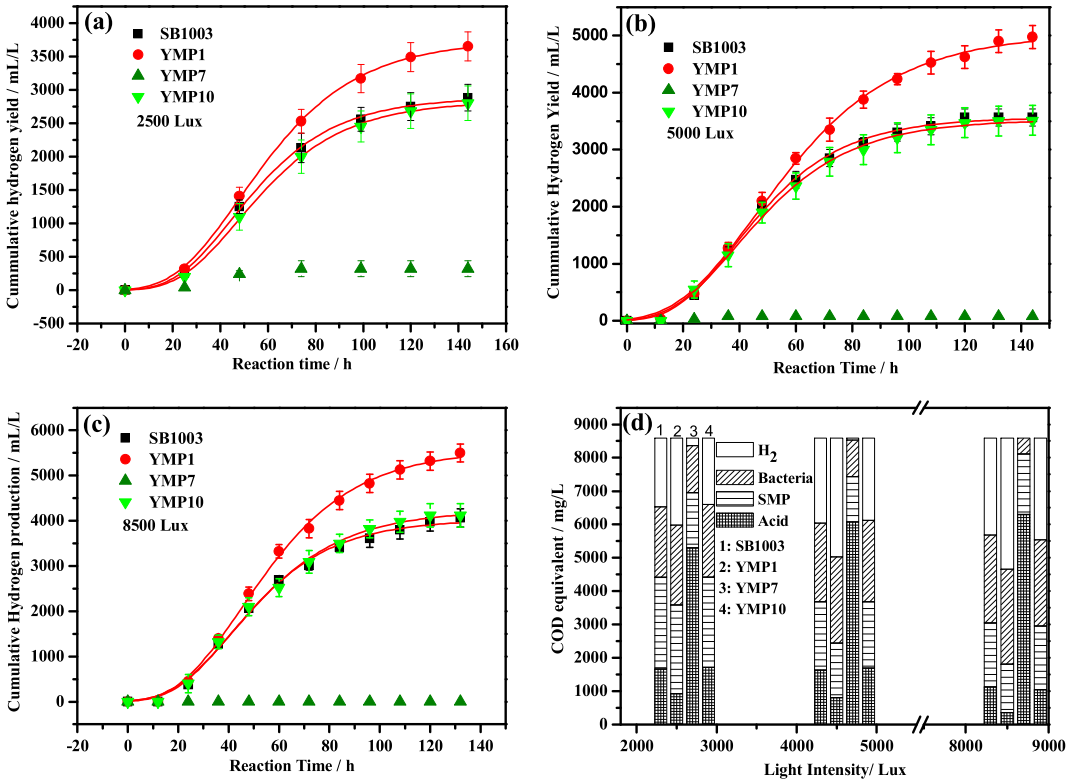

Fig. 2 – Cumulative of hydrogen yields of YMP1, SB1003, YMP7 and YMP10 from photo-fermentation under the light intensity of 2500 ± 300 lux (a), 5000 ± 300 lux (b) and 8500 ± 500 lux (c), and the diversity of substrate conversion in the end products of hydrogen, bacterial biomass, soluble microbial products and retained acetic and butyric acids, which were showed in the manner of chemical oxygen demand calculated according to the hydrogen yields or determined by COD measurements (d). The scatters in (a), (b) and (c) represent the experimental data and the lines were obtained by fitting with modified Gompertz equation.

when the light intensity was increased to 8000 lux [25], and they believed that the decrease of hydrogen production performance at high light intensity was caused by the excessive light intensity. When YMP1(*mopAB*$^{-}$) was employed for hydrogen production under the same conditions, the increase ratio of its maximum hydrogen production rate was 39.8% when the light intensity was increased from 2500 ± 300 lux to 5000 ± 300 lux, and it was increased clearly by 17.6% even when the light intensity was increased from 5000 ± 300 lux into 8500 ± 500 lux. Although the increase ratio of hydrogen production rate was lower than that of light intensity, it increased clearly when Fe-nitrogenase and Mo-nitrogenase were co-expressed in the *mopAB*-disrupted mutant. The YMP10 showed slightly lower hydrogen production rates compared with SB1003, and this result also indicate the enhancement of hydrogen production rate in YMP1 was attribute to the synergistic function of Mo- and Fe-nitrogenase, but not other positive effects caused by *mopAB* disruption.

These data suggest that the light energy could be a limited factor for hydrogen production at low light intensity. At low light intensity, the light absorption by bacteria could be a limited factor for hydrogen production since nitrogenase demands ATP that is mainly synthesized by photophosphorylation. At high light intensity, the ATP synthesis is no longer a limited factor, but the activity of nitrogenase could limit the hydrogen production rate and therefore cause energy waste and even damage to the bacteria, and this was the reason for the more remarkable enhancement of hydrogen production rate of YMP1 compared with that of SB1003. In the *mopAB*-disrupted mutant, the co-expression of Mo- and Fe-nitrogenase enhanced the hydrogen production activity. The increased nitrogenase activity determined by acetylene reducing method shown in Table 3 revealed that the two nitrogenase systems functioned synergistically in YMP1 strain, and therefore enhanced the hydrogen yield and maximum hydrogen production rate. In YMP7 (Δ*nifHD*, Δ*mopAB*) mutant, only the Fe-nitrogenase is functional, and the activity of this nitrogenase system is relatively lower at 0.47 ± 0.19 nmol acetylene/(min·mg-dry cells) compared with that of 2.97 ± 0.20 nmol acetylene/(min·mg-dry cells) dedicated by the Mo nitrogenase in wild type strain as shown in Table 3. At low light intensity of 2500 ± 300 lux, a hydrogen yield of 320 ± 120 mL/L was obtained, and when the light intensity was increased, the increase of input light energy might be harmful to the bacteria. Although the CO_2 fixation cycle was functioning, the function of this pathway on dissipating the reducing force is dependent on the reducing state of the carbon sources. In this study, the carbon sources was composed of 25 mM acetic acid and 30 mM butyric acid, which

showed lower reducing state than that of bacteria biomass. Therefore, hydrogen production was a significant way for dissipating the redundant energy, and the lower nitrogenase activity led to negligible hydrogen yield and poor growth. The purified Fe-nitrogenase prepared by Müller et al. showed comparable hydrogen production activity with that of the purified Mo-nitrogenase [24], and it is found that the Fe-nitrogenase is naturally more favorable for hydrogen production under nitrogen fixation condition compared with conventional Mo-nitrogenase [17], the data obtained in this work suggested the single Fe-nitrogenase system showed much lower hydrogen production activity compared with that of Mo-nitrogenase in vivo, and the single Fe-nitrogenase is hard to support efficient hydrogen production. Co-expression of two nitrogenase system could clearly enhance the hydrogen production performance both on hydrogen yield and hydrogen production rate.

Fig. 2(d) shows the diversity of substrate during the photo-fermentation. In general, the substrate including carbon sources, nitrogen source in the culture was converted into hydrogen, bacterial biomass, soluble microbial products (SMP), and some of the carbon sources were remained in the culture. All the amounts of these components were calculated into or determined by the chemical oxygen demand values (COD) and marked as COD equivalent value (COD_{eq}) shown in Fig. 2(d). The remained acetic and butyric acids concentrations showed by COD_{eq} in SB1003 culture were decreased from 1666.7 mg/L into 1639 mg/L and 1131.2 mg/L when the light intensity was increased. And in YMP1, the remained acids concentrations in COD_{eq} were decreased from 923.6 mg/L to 803.9 mg/L and 358.1 mg/L with the increase of light intensity. While in YMP7 cultures, most of the acetic and butyric acids were retained, and the bacteria were grown poorly, which were around 0.96 g-dcw/L, 0.75 g-dcw/L and 0.32 g-dcw/L respectively when the light intensity was enhanced. For the amounts of SMP, it decreased from 2747.1 mg/L in COD_{eq} to 2048.9 mg/L and 1916.2 mg/L in the wild type strain culture along with the increase of light intensity. These results indicate that the amount of substrate converted into SMP was decreased when the light intensity was increased, and meanwhile, the hydrogen yield was increased. In the YMP1 cultures, the SMP concentrations were 2661.2 mg/L, 1642.5 mg/L and 1457.5 mg/L at the light intensity from low to high order. These results also indicate that at low light intensity, more substrates were converted into SMP due to the limitation of nitrogenase activity. In YMP10 culture, it showed similar hydrogen production performance and SMP profiles with the wild type strain SB1003.

Conclusions

The expression level of Mo-nitrogenase was not negatively affected in YMP1, and the nitrogenase activity of YMP1 determined by acetylene reducing method was 4.22 ± 0.30 nmol acetylene/(min·mg-dry cells), which was clearly higher than that of 2.97 ± 0.20 nmol acetylene/(min·mg-dry cells) obtained in the wild type strain. The tests of photo-fermentative hydrogen production showed that the maximum hydrogen production rates of YMP1 under different light intensity were clearly higher than those of wild type strain. Fe-nitrogenase could not support efficient photosynthetic hydrogen production alone, but it showed synergistic effect with Mo-nitrogenase on hydrogen production when they were co-expressed.

Acknowledgments

The authors appreciate Dr. Chen Guoqiang from Tsinghua University and Dr. Fevzi Daldal from University of Pennsylvania for offering some plasmids. We acknowledge the financial support from National Natural Science Foundation of China for the Youth (No. 51308452) and the National Basic Research Program of China (No. 2012CB215303). One of the authors (HY) was financially supported by the Specialized Research Fund for the Doctoral Program of Higher Education (No. 20120201120058) and "The Fundamental Research Funds for the Central University" (No. 08143066).

REFERENCES

[1] Ma C, Yang H, Zhang Y, Guo L. Disruption of multidrug resistance protein gene of *Rhodobacter capsulatus* results in improved photoheterotrophic hydrogen production. Int J Hydrogen Energy 2013;38(29):13031–7.
[2] Abo-Hashesh M, Desaunay N, Hallenbeck PC. High yield single stage conversion of glucose to hydrogen by photofermentation with continuous cultures of *Rhodobacter capsulatus* JP91. Bioresour Technol 2013;128(0):513–7.
[3] Wang Y-Z, Liao Q, Zhu X, Chen R, Guo C-L, Zhou J. Bioconversion characteristics of *Rhodopseudomonas palustris* CQK 01 entrapped in a photobioreactor for hydrogen production. Bioresour Technol 2013;135(0):331–8.
[4] Wang X, Yang H, Ma C, Guo L. Enhanced photosynthetic hydrogen production performance of *Rhodobacter capsulatus* by deactivating CBB cycle and cytochrome c oxidase. Int J Hydrogen Energy 2014;39(7):3176–84.
[5] Yang H, Zhang J, Wang X, Jiangtao F, Yan W, Liejin G. A newly isolated *Rhodobacter sphaeroides* HY01 with high hydrogen production performance. Int J Hydrogen Energy 2014;39(19):10051–60.
[6] Yang H, Wang X, Zhang L, Guo L. Enhanced hydrogen production performance of *Rubrivivax gelatinosus* M002 using mixed carbon sources. Int J Hydrogen Energy 2012;37(18):13296–303.
[7] Lo S-C, Shih S-H, Chang J-J, Wang C-Y, Huang C-C. Enhancement of photoheterotrophic biohydrogen production at elevated temperatures by the expression of a thermophilic *clostridial* hydrogenase. Appl Microbiol Biotechnol 2012;95(4):969–77.
[8] Cai J, Wang G. Screening and hydrogen-producing characters of a highly efficient H_2-producing mutant of *Rhodovulum sulfidophilum* P5. Bioresour Technol 2013;142(0):18–25.
[9] Kars G, Gündüz U, Rakhely G, Yücel M, Eroglu I, Kovacs KL. Improved hydrogen production by uptake hydrogenase deficient mutant strain of *Rhodobacter sphaeroides* O.U.001. Int J Hydrogen Energy 2008;33(12):3056–60.
[10] Kim M-S, Kim D-H, Son H-N, Ten LN, Lee JK. Enhancing photo-fermentative hydrogen production by *Rhodobacter sphaeroides* KD131 and its PHB synthase deleted-mutant from acetate and butyrate. Int J Hydrogen Energy 2011;36(21):13964–71.

[11] Yang C-F, Lee C-M. Enhancement of photohydrogen production using *phbC* deficient mutant *Rhodopseudomonas palustris* strain M23. Bioresour Technol 2011;102(9):5418–24.
[12] Wang D, Zhang Y, Welch E, Li J, Roberts GP. Elimination of Rubisco alters the regulation of nitrogenase activity and increases hydrogen production in *Rhodospirillum rubrum*. Int J Hydrogen Energy 2010;35(14):7377–85.
[13] Wang X, Yang H, Zhang Y, Guo L. Remarkable enhancement on hydrogen production performance of *Rhodobacter sphaeroides* by disrupting spbA and hupSL genes. Int J Hydrogen Energy 2014;39(27):14633–41.
[14] Ozturk Y, Gokce A, Peksel B, Gurgan M, Ozgur E, Gunduz U, et al. Hydrogen production properties of *Rhodobacter capsulatus* with genetically modified redox balancing pathways. Int J Hydrogen Energy 2012;37(2):2014–20.
[15] Wang G, Angermüller S, Klipp W. Characterization of *Rhodobacter capsulatus* genes encoding a molybdenum transport system and putative molybdenum-pterin-binding proteins. J Bacteriol 1993;175(10):3031–42.
[16] Müller A, Püttmann L, Barthel R, Schön M, Lackmann J-W, Narberhaus F, et al. Relevance of individual Mo-box nucleotides to DNA binding by the related molybdenum-responsive regulators MopA and MopB in *Rhodobacter capsulatus*. FEMS Microbiol Lett 2010;307(2):191–200.
[17] McKinlay JB, Harwood CS. Photobiological production of hydrogen gas as a biofuel. Curr Opin Biotechnol 2010;21(3):244–51.
[18] Yen HC, Marrs B. Map of genes for carotenoid and bacteriochlorophyll biosynthesis in *Rhodopseudomonas capsulata*. J Bacteriol 1976;126(2):619–29.
[19] Daldal F, Cheng S, Applebaum Joy, Davidson Edgar, Prince Roger C. Cytochrome c2 is not essential for photosynthetic growth of *Rhodopseudomonas capsulata*. Proc Natl Acad Sci U S A 1986;83(7):2012–6.
[20] Sistrom WR. A Requirement for Sodium in the Growth of *Rhodopseudomonas spheroides*. J Gen Microbiol 1960;22(3):778–85.
[21] Ditta G, Stanfield S, Corbin D, Helinski DR. Broad host range DNA cloning system for gram-negative bacteria: construction of a gene bank of *Rhizobium meliloti*. Proc Natl Acad Sci U S A 1980;77(12):7347–51.
[22] Adams CW, Forrest ME, Cohen SN, Beatty JT. Structural and functional analysis of transcriptional control of the *Rhodobacter capsulatus puf* operon. J Bacteriol 1989;171(1):473–82.
[23] Chen C-Y, Lu W-B, Liu C-H, Chang J-S. Improved phototrophic H_2 production with *Rhodopseudomonas palustris* WP3–5 using acetate and butyrate as dual carbon substrates. Bioresour Technol 2008;99(9):3609–16.
[24] Schneider K, Gollan U, Dröttboom M, Selsemeier-Voigt S, Müller A. Comparative biochemical characterization of the iron-only nitrogenase and the molybdenum nitrogenase from *Rhodobacter capsulatus*. Eur J Biochem 1997;244(3):789–800.
[25] Wang J, Wan W. Kinetic models for fermentative hydrogen production: a review. Int J Hydrogen Energy 2009;34(8):3313–23.
[26] Yano T, Sanders C, Catalano J, Daldal F. sacB–5-Fluoroorotic Acid–pyrE-based bidirectional selection for integration of unmarked alleles into the chromosome of *Rhodobacter capsulatus*. Appl Environ Microbiol 2005;71(6):3014–24.
[27] Kovach ME, Elzer PH, Steven Hill D, Robertson GT, Farris MA, Roop Ii RM, et al. Four new d erivatives of the broad-host-range cloning vector pBBR1MCS, carrying different antibiotic-resistance cassettes. Gene 1995;166(1):175–6.